Letters in Applied NanoBioScience
Open-Access Journal (ISSN: 2284-6808)

Article
Volume 13, Issue 4, 2024, 168
https://doi.org/10.33263/LIANBS134.168

pH-Sensitive CNC-Chitosan Hydrogel for Drug Delivery

Felycia Edi Soetaredjo [1,2], Suryadi Ismadji [1,2,*], Shella Permatasari Santoso [1,2], Jindrayani Nyoo Putro [1,2], Kuncoro Foe [3], Gladdy L. Waworuntu [4]

[1] Department of Chemical Engineering, Widya Mandala Surabaya Catholic University; shella@ukwms.ac.id (S.P.S.); jindrayani@ukwms.ac.id (J.Y.P.);
[2] Collaborative Research Center for Zero Waste and Sustainability, Jl. Kalijudan 37, Surabaya 60114, East Java, Indonesia; shella@ukwms.ac.id (S.P.S.); jindrayani@ukwms.ac.id (J.Y.P.);
[3] Faculty of Pharmacy, Widya Mandala Surabaya Catholic University, Kalisari Selatan No.1 Kalisari, Surabaya 60112, Indonesia; kuncoro@ukwms.ac.id (K.F.);
[4] Faculty of Medicine, Widya Mandala Surabaya Catholic University, Kalisari Selatan No.1 Kalisari, Surabaya 60112, Indonesia; gladdy@ukwms.ac.id (G.L.W.);
* Correspondence: suryadiismadji@yahoo.com (S.I.); felyciae@yahoo.com (F.E.S.)

Scopus Author ID 10039423500
Received: 14.09.2023; Accepted: 7.07.2024; Published: 25.08.2024

Abstract: In contemporary society, inflammatory bowel disease (IBD) is prevalent and acknowledged. In treating inflammatory bowel disease (IBD), pH-sensitive drug delivery systems are commonly utilized. Nonetheless, their efficacy tends to be reduced as a result of modifications in the pH levels within the intestines. This study aims to develop a medication delivery system responsive to changes in pH to deliver 5-aminosalicylic acid specifically to the colon. CNC-chitosan hydrogel was produced by implementing the cross-linking technique, employing glutaraldehyde as the cross-linking agent. The hydrogel was subjected to characterization using scanning electron microscopy (SEM), X-ray diffraction (XRD), swelling capacity analysis, and Fourier-transform infrared spectroscopy (FTIR). The release kinetics of 5-aminosalicylic acid from cellulose nanocrystals (CNC) and CNC-chitosan composites showed superior performance at pH 7.4 compared to pH 2.4. The release profile of 5-aminosalicylic acid from CNC-chitosan hydrogel can be accurately represented by the Korsemeyar-Peppas equation. CNC and CNC-chitosan were compatible with osteoblast cells, indicating their lack of toxicity.

Keywords: sustained-release; hydrogel; inflammatory bowel disease.

1. Introduction

Inflammatory bowel disease (IBD) is inflammation of the intestines, particularly the large intestine. This disorder is widely observed and recognized in modern culture [1]. Ulcerative colitis and Crohn's disease are two subtypes of IBD [2]. The development of this condition can be attributed to various causes, including heredity, an imbalanced lifestyle, an erratic dietary pattern, geographical location, and a compromised immune system [3]. Treatment of IBD often involves the use of pH-sensitive drug delivery systems. However, their effectiveness is typically compromised due to alterations in intestinal pH.

Several medications, such as sulfasalazine, 5-aminosalicylic acid, budesonide, corticosteroids, thiopurines, and methotrexate, have been identified as potential therapeutic options for managing this medical condition [4]. The effectiveness of this medication presents difficulties for individuals. One notable challenge is that certain medicines used to treat colitis are rapidly absorbed in the small intestine, resulting in limited quantities reaching the large

intestine. Moreover, various additional formulations of the medication can potentially induce adverse consequences, such as the development of colon cancer. Some inherited disorders, including pancreatitis, hepatitis, blood dyscrasias, and interstitial nephritis, may also manifest [5].

Several drug delivery techniques have been created to address the challenges associated with medication administration. These improvements include the utilization of natural or synthetic polymer-based nanoparticles for targeted or regulated release [6, 7]. Due to their inherent benefits over conventional drug delivery methods, intelligent drug delivery systems have garnered significant academic attention. It is widely considered that intelligent drug delivery systems have the potential to enhance the efficacy of drugs, minimize effects, and augment pharmacological activity. A sustained-release mechanism stands out as a particularly promising approach [8–10].

Several drug carriers have been established for sustained-release systems, with hydrogels emerging as the predominant choice among them. Hydrogels have a distinctive characteristic: they can undergo swelling and absorb substantial water. This feature serves as a protective mechanism for drug molecules within the human body, shielding them from adverse conditions and reducing the risk of drug denaturation before reaching their designated target site. Hydrogels possess a three-dimensional porous network architecture, enabling them to regulate the drug release rate via swelling mechanisms or in response to variations in pH within the human body. This mechanism results in the controlled and consistent release of the medication from the hydrogel, thereby minimizing drug toxicity and the risk of overdose [8].

Numerous global research organizations have investigated synthesizing hydrogels to achieve prolonged drug release. These studies have involved the utilization of natural polymers in conjunction with a diverse range of organic components as linkers [10–15]. The primary obstacle in developing hydrogels for sustainable drug release lies in the use of volatile and hazardous solvents, cross-linking chemicals, and initiators, which pose significant risks to human health and the environment. Hence, it is imperative to exert more effort to develop environmentally sustainable hydrogels derived from natural resources.

The present study employed a synthesis approach to produce a hydrogel using natural constituents, including crystalline nanocellulose (CNC), chitosan, and carboxyl methylcellulose. Utilizing these natural ingredients in producing hydrogels yields biocompatible, biodegradable, non-toxic, hydrophilic products with a high water absorption capacity. The hydrogel served as a medium for the controlled release of 5-aminosalicylic acid medicines within the colon. The hydrogel material was also engineered to exhibit sensitivity to changes in the pH of the surrounding solution. The investigation focused on the prolonged release of 5-aminosalicylic acid from the hydrogel at two distinct pH levels: 7.4, which represents simulated intestinal fluid, and 2.4, which represents simulated stomach fluid.

2. Materials and Methods

2.1. Materials.

The CNC used in this investigation was derived from durian shells. The CNC extraction was conducted with a 56% sulfuric acid solution at 30°C. Details of CNC extraction can be seen elsewhere [16]. Chitosan (medium molecular weight, CAS no. 9012-76-4), 5-aminosalicylic acid ($H_2NC_6H_3$-2-$(OH)CO_2H$, ≥ 99%), acetic acid (CH_3COOH, 99%), and Glutaraldehyde ($OHC(CH_2)_3CHO$, 8%) were purchased from Sigma Aldrich. The additional

chemicals used in this study were procured from a regional chemical supplier in Surabaya, Indonesia. The water used for washing and as a solvent was reverse osmosis (RO) water, which has a maximum concentration of total dissolved solids (TDS) at six parts per million (ppm).

2.2. Preparation of CNC-chitosan hydrogels composite.

Several procedures were employed in the preparation of the CNC-chitosan hydrogel. In the first step, a certain quantity of chitosan was introduced into a solution of acetic acid with a concentration of 5% (v/v), forming a chitosan solution with a concentration of 2% (w/v). During the dissolution process, agitation was performed at 200 rpm for 12 hours at a rotational speed. Subsequently, a certain quantity of CNC was introduced into a solution containing 2% chitosan, forming a mixture with a CNC concentration of 2.5% (w/v). During the mixing process, the mixture was stirred at a consistent rotational speed of 200 revolutions per minute (rpm) for 2 hours to ensure the uniformity and homogeneity of the mixture. A solution containing 0.2% (v/v) of glutaraldehyde was introduced to the CNC-chitosan combination and agitated at 250 rpm for 2 hours. Subsequently, the mixture was transferred into a petri dish and subjected to a drying process lasting for 24 hours.

2.3. Characterization of CNC-chitosan hydrogel.

The drug release process is significantly influenced by the swelling capacity of the CNC-chitosan hydrogel at various pH levels when employed as a drug carrier. Hence, an investigation was conducted to examine the swelling capacity of CNC-chitosan under two distinct pH conditions, namely pH 2.4 (representing gastric fluid) and pH 7.4 (representing intestinal fluid). The CNC-chitosan sample was dried at 50°C until a consistent weight was achieved. Following this, the CNC-chitosan material was submerged in a buffer solution, and the weight of the enlarged hydrogen was measured periodically for up to 72 hours. The swelling ratio (SwR) can be determined by employing the subsequent mathematical expression:

$$SwR = \frac{W_s - W_o}{W_o} x100\% \qquad (1)$$

W_s is the weight of swollen CNC-chitosan, and W_o is the initial weight of CNC-chitosan.

A scanning electron microscope (SEM) study acquired the CNC-chitosan hydrogel surface topography. The JEOL JSM-6500F field emission scanning electron microscopy instrument performed the investigation. The samples' crystallinity degree was assessed using the X-ray diffraction (XRD) technique of the Philips PANalytical X'Pert X-ray powder diffractometer. The surface functional groups of the samples were determined by employing the Fourier Transform Infrared (FTIR) approach utilizing the Shimadzu 8400S FTIR instrument.

2.4. Drug loading and release studies.

To prepare a 5-aminosalicylic acid solution with a concentration of 250 mg/L, 25 mg of 5-aminosalicylic acid is dissolved in 100 mL of water. After adding 100 mg of cellulose nanocrystals (CNC) or CNC-chitosan to the solution containing 5-aminosalicylic acid, the mixture was sonicated for 5 minutes. The mixture was then transferred to a water bath shaker and shaken at a controlled temperature of 30°C for 6 hours at 100 rpm. After the adsorption process reached equilibrium, the CNC or CNC-chitosan particles containing 5-aminosalicylic acid were separated by centrifugation and then dried under a vacuum. Using a UV-vis

spectrophotometer with a wavelength of 450 nm, the concentration of 5-aminosalicylic acid remaining in solution was then measured.

The release of 5-aminosalicylic acid from CNC or CNC-chitosan, both of which are pre-loaded with 5-aminosalicylic acid, was achieved by applying the membrane dialysis technique. Particles containing 5-aminosalicylic acid in 5 mL of simulated intestinal fluid (pH 7.4) or simulated gastric fluid (pH 2.4) were added to the dialysis tube (MWCO = 14,000 Da). The dialysis tube was placed in a beaker containing 95 mL of simulated intestinal or gastric fluid. The drug release experiment was carried out at 37°C. At specified time intervals, 5 mL of the solution was withdrawn from the system, and simultaneously, an equal volume of fresh simulated intestinal or gastric fluid solution was added to the system. The concentration of 5-aminosalicylic acid in simulated intestinal or gastric fluid solutions was determined using a UV-vis spectrophotometer.

2.5. Cell viability study.

The effectiveness and compatibility tests of CNC and CNC-chitosan were conducted using the MMT method. Cell viability assays were performed using the 7F2 cell line. A dose-response curves were prepared by treating the 7F2 cell line with CNC, chitosan-CNC, 5-aminosalicylic acid-loaded CNC, 5-aminosalicylic acid-loaded CNC-chitosan, and as a control, the 7F2 cell line was prepared without treatment. CNCs, CNCs-chitosan, 5-aminosalicylic acid-loaded CNCs, and 5-aminosalicylic acid-loaded CNCs-chitosan were evaluated at 0.25 mg/mL for treatment. Prior to the MMT (3-(4,5-dimethylthiazol-2-yl)-2,5-diphenyltetrazolium bromide) assay, cells were rinsed with simulated intestinal or gastric fluids, and MMT working solution was added, and incubated at 37°C for four hours. MMT was converted to formazan during cell viability assays. The formazan crystals were dissolved using a DMO solution.

3. Results and Discussion

3.1. Characterization of CNC-chitosan hydrogel.

Swelling experiments for CNC-chitosan hydrogel were carried out using RO water, simulated gastric fluid, and simulated intestinal fluid as immersion mediums. As shown in Figure 1, the swelling percentage of CNC-chitosan increased with increasing immersion time for all mediums. Figure 1 shows that CNC-chitosan hydrogel displayed rapid swelling, surpassing 100 percent swelling percentage within a mere 20 minutes when immersed in RO water or intestinal fluid.

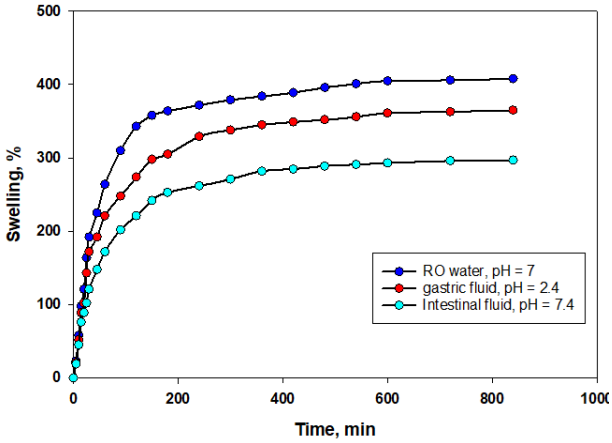

Figure 1. The swelling ratio of CNC-chitosan hydrogel.

The fast swelling property indicates that capillary force is more dominant than water absorption. Generally, hydrogels have large pores (up to hundreds of micrometers), acting like a capillary system so that water can be absorbed easily [18]. As depicted in Figure 1, the presence of salts in the simulated gastric and intestinal fluids affects the swelling ability of the CNC-chitosan hydrogel.

The topography of the CNC and CNC-chitosan hydrogel surfaces can be seen in Figure 2. This figure shows the typical rod-shaped structure of CNC (Figure 2a). In contrast, the distinctive CNC shape is no longer visible in the hydrogel (Figure 2b), indicating that the CNC has been thoroughly mixed with the chitosan to form a homogeneous hydrogel. The surface of the resulting hydrogel is relatively smooth.

Figure 2. SEM images of **(a)** CNC; **(b)** CNC-chitosan hydrogel.

The X-ray diffraction (XRD) technique was employed to obtain the XRD patterns of cellulose nanocrystals (CNC), pristine chitosan, and the CNC-chitosan hydrogel (Figure 3). The XRD pattern of CNC has five distinct peaks at 2θ values of 15.2°, 16.4°, 20.4°, 22.6°, and 34.8°. The observed peaks correspond to the crystallographic planes ($\bar{1}10$), (110), (102), (200), and (004). These Miller indices suggest the presence of the cellulose I structure [17].

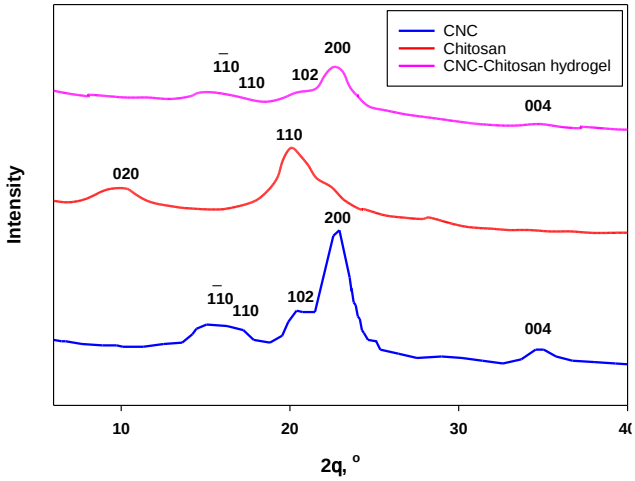

Figure 3. XRD diffractograms of CNC, chitosan, and CNC-chitosan hydrogel.

Chitosan is generated from chitin by the deacetylation process, which involves the treatment of chitin with alkali before deacetylation. Chitosan has a crystalline polymer nature with a molecular structure resembling cellulose. Notably, most of its secondary hydroxyl groups are substituted with amino groups. Chitosan has a distinctive characteristic on the X-ray diffraction (XRD) diffractogram, namely the presence of two broad peaks at 2θ of 10.1° and 20°. The observed peaks in the chitosan lattice crystalline correspond to the Miller indices (020) and (110) [17]. The disappearance of these distinctive peaks can be attributed to the potential substitution of hydroxyl and amino groups with glutaraldehyde during cross-linking.

The diffraction peaks observed in the CNC chitosan hydrogel were found at 2θ 14.8°, 16.3°, 20.4°, 22.3°, and 34.4°. These peaks exhibited a somewhat diminished intensity, suggesting a weakening of the CNC crystal structure. Additionally, the diffraction pattern shifted towards lower angles, indicating a reduction in the CNC crystal structure due to the inclusion of chitosan. The findings of this study demonstrate that the CNC-chitosan hydrogel exhibits a combination of amorphous and crystalline regions.

Table 1 displays the functional groups of CNC, chitosan, and CNC-chitosan hydrogel as determined by the Fourier Transform Infrared (FTIR) technique. FTIR analysis revealed several functional groups of chitosan. Specifically, wave numbers 3357 cm^{-1} and 2905 cm^{-1} correspond to the overlapping of the O–H stretching and N–H stretching vibrations and C–H asymmetric stretching vibration [18]. C=O stretching of amide I was observed at wavenumber 1642 cm^{-1}, while NH bending of primary amine was found at 1588 cm^{-1}. Peaks at wavenumbers 1424 and 1373 cm-1 wavenumbers belong to CH_3 symmetrical deformations and CH_2 bending [18].

Table 1. Surface functional groups of CNC, chitosan, and CNC-chitosan hydrogel.

Surface functional groups	CNC Wavenumber, 1/cm	Chitosan Wavenumber, 1/cm	CNC-chitosan Wavenumber, 1/cm
overlapping of the O–H stretching and N–H stretching vibrations	-	3357	3338
C–H asymmetric stretching vibration	-	2874	2905
C=O stretching of amide I	-	1642	-
stretching vibrations of C=N	-	-	1551
NH bending of primary amine	-	1588	-
CH_3 symmetrical deformations	-	1424	1408
CH_2 bending	-	1373	-
C-N stretching of amide III	-	1320	
Asymmetric stretching of the C–O–C bridge	-	1155	-
C–O stretching of the C-3 position	-	1061 and 1031	-
stretching vibration of the C–H	2904	-	2905
O–H deformation	1643	-	1645
β-glycosidic bond vibration	898	-	895
Iβ-type cellulose	712	-	-
Iα-type cellulose	748	-	-

The functional groups of the CNCs were determined by analyzing the characterization results using FTIR. The absorbance observed at a wave number of 2904 cm^{-1} corresponds to the stretching vibration of the C–H functional group. The O–H deformation functional group exhibits a characteristic absorption peak at a wave number 1643 cm^{-1}. The cellulose amorphous component within the CNC was identified by observing a peak at a wave number of 898 cm^{-1}, corresponding to the vibrational frequency of a β-glycosidic bond. The absorption peak observed for Iβ-type cellulose was recorded at a wavenumber of 710 cm^{-1}, while for Iα-type cellulose, the absorption peak was observed at 750 cm^{-1} [19]. Following the formation of the CNC-alginate hydrogel, a noticeable alteration in the wave numbers of many peaks was observed, as depicted in Table 1. A new peak at a wave number of 1551 cm^{-1} signifies the formation of cross-links between the amino groups of chitosan and the aldehyde groups of glutaraldehyde.

3.2. Drug loading and release studies.

The experimental findings revealed that the CNC exhibited a maximum adsorption capacity of 67.8 mg/g for 5-aminosalicylic acid, whereas the CNC-chitosan hydrogel showed

a higher adsorption capacity of 93.6 mg/g. The prediction of drug release from a solid matrix through the utilization of both simple and complex mathematical equations represents a formidable task within the field of drug delivery. Such models are commonly used to accelerate the design process of pharmaceutical formulations and verify drug release mechanisms within the human body.

The Higuchi model is the most commonly used equation among the various models that describe drug release kinetics [20-25]. The subsequent mathematical model is the Higuchi equation:

$$\frac{n_t}{n_{max}} = k_H\sqrt{t} \qquad (2)$$

The parameter k_H represents the Higuchi constant with a well-defined and realistic physical interpretation. The symbol n_t denotes the cumulative drug release at time t, whereas n_{max} represents the maximum amount of drug that can be delivered over an infinite duration.

The Korsemeyar-Peppas equation frequently represents drug release data in various systems [20-24]. The mathematical expression of the Korsmeyer-Peppas equation is as follows:

$$\frac{n_t}{n_{max}} = k_{KP}t^n \qquad (3)$$

The Korsemeyar-Peppas constant, denoted as k_{KP}, is a parameter used in drug release studies. The diffusion exponent, represented by the symbol n, is a feature that describes the transport mechanism involved in the release of the drug.

In many instances, the drug release profile in specific systems has a sigmoidal form, rendering the generally employed equations inadequate to describe the kinetics of drug release accurately. To address this limitation, a mathematical model based on actual data was constructed to describe the release of drugs in a sigmoidal pattern [16], as given in Equation 4.

$$\frac{n_t}{n_{max}} = \frac{R_{max}}{(1+exp(-(t-t_{50})/k_s))} \qquad (4)$$

The parameter R_{max} represents the upper limit of the theoretical release, whereas k_s denotes the constant rate at which the release occurs. The parameter t_{50} denotes the duration the system releases 50 percent of its maximum output.

The release of 5-aminosalicylic acid from CNC and CNC-chitosan was conducted in two distinct release media, namely simulated intestinal fluid with a pH of 7.4 and simulated gastric fluid with a pH of 2.4. Figure 4 illustrates the percentage release of 5-aminosalicylic acid from cellulose nanocrystals (CNC) and CNC-chitosan as a function of time under two distinct pH conditions.

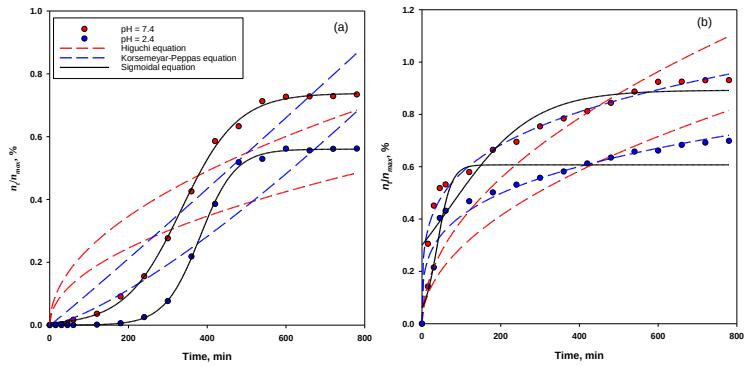

Figure 4. 5-aminosalicylic acid release profile from **(a)** CNC; **(b)** CNC-chitosan.

The release of the drug from CNC-alginate exhibited a biphasic pattern, characterized by an initial quick release (referred to as the burst effect) followed by a continuous release. The fast release of 5-aminosalicylic acid in CNC-chitosan hydrogel at pH 7.4 and 2.4 was detected

within the first 45 minutes, during which 40-50% of the medication was released. Subsequently, a steady release of the drug was observed from 45 to 480 minutes. The burst effect reported in this study is likely attributed to the release of 5-aminosalicylic acid, which was adsorbed onto the surface of CNC-chitosan. The sustained release of 5-aminosalicylic acid was facilitated by the diffusion of the drug from the inside pore of the hydrogel towards its surface, followed by further diffusion into the surrounding liquid medium.

In the context of controlled-release drug delivery systems, it was observed that the release of 5-aminosalicylic acid in a cellulose nanocrystal matrix exhibited a slow-release profile. Specifically, the quantity of drug released into the simulated solution was below 4% within the initial 120-minute timeframe. The structure of CNC differs from that of CNC-chitosan hydrogel. CNC exhibits a high degree of physical entanglement and attractive interaction with 5-aminosalicylic acid, impeding the drug's release into the simulated fluid.

The release kinetics of 5-aminosalicylic acid from cellulose nanocrystals (CNC) and CNC-chitosan composites showed superior performance at pH 7.4 compared to pH 2.4. At a pH of 7.4, the efficiency of the release of 5-aminosalicylic acid from cellulose nanocrystals (CNC) was around 73%, whereas at a pH of 2.4, it was only approximately 56%. The release effectiveness of 5-aminosalicylic acid is superior when using CNC-chitosan hydrogel compared to CNC. The drug release efficacy is approximately 93% at a pH of 7.4 and 70% at a pH of 2.4. The dissimilar release profiles of 5-aminosalicylic acid exhibited by the two materials can be attributed to variances in structural features such as functional groups, crystallinity, and swelling properties. CNC-chitosan possesses a more significant number of hydroxyl (OH) groups than CNC, resulting in an increased presence of OH groups that can facilitate hydrogen bonding. The propensity of CNC-chitosan hydrogel to bind water is higher than that of 5-aminosalicylic acid, resulting in its facile release into the solution.

The Higuchi equation does not adequately represent the kinetic data of 5-aminosalicylic acid release from CNCs and CNC-chitosan hydrogels, as depicted in Figure 4. The rationale behind simplifying the existing phenomena has been largely addressed during the formulation of the Higuchi equation. Therefore, it is unsurprising that the Higuchi equation fails to describe drug release kinetics in various systems accurately. Drug release from swellable systems often encompasses Fickian diffusion, water transport, and relaxational swelling. These characteristics can be well described by the Korsemeyar-Peppas equation. Although the equation in question does not thoroughly depict the release of 5-aminosalicylic acid from CNC, it has been found that the Korsemeyar-Peppas equation may effectively model the release of 5-aminosalicylic acid from CNC-Chitosan hydrogels.

3.3. Cell viability study.

The outcomes of the biocompatibility assessment of CNC and CNC-chitosan with a 7F2 cell line are depicted in Figure 5. The results depicted in Figure 5 provide evidence of the biocompatibility of CNC and CNC-chitosan with osteoblast cells, indicating their lack of toxicity. The graph presented in this study illustrates that the increased cell viability observed in CNC and CNC-chitosan hydrogels may be attributed to the reduced diffusion rate of CNC and CNC-chitosan from the surface towards the cells.

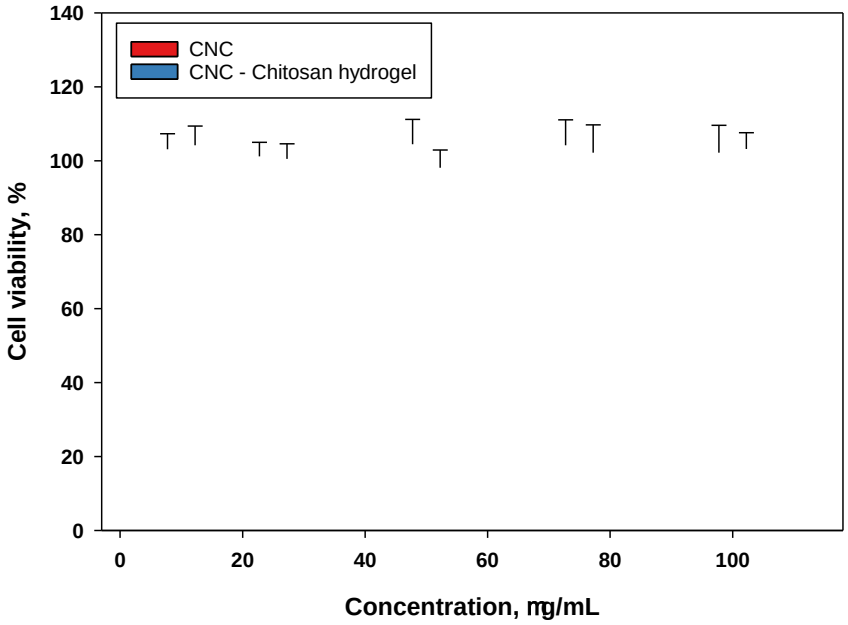

Figure 5. Cell viability of CNC and CNC-chitosan hydrogel.

4. Conclusions

The present study effectively employed acid hydrolysis to extract cellulose nanocrystals (CNC) from durian shell waste. The present study elucidated how agricultural waste can be transformed into materials with enhanced value using a simplified approach. The current investigation utilized a synthetic methodology to produce a hydrogel by including naturally occurring components, namely crystalline nanocellulose (CNC), chitosan, and carboxyl methylcellulose. Utilizing these naturally occurring substances in producing hydrogels creates biocompatible, biodegradable, non-toxic, and hydrophilic materials with a significant capacity for water absorption. The hydrogel is a substrate for the regulated delivery of 5-aminosalicylic acid pharmaceuticals within the colonic region. The drug's release from CNC-alginate demonstrated a biphasic pattern, consisting of an initial rapid release (often known as the burst effect) followed by a sustained release. The performance of the release kinetics of 5-aminosalicylic acid from cellulose nanocrystals (CNC) and CNC-chitosan composites was superior at pH 7.4 compared to pH 2.4. The Higuchi equation fails to accurately depict the kinetic data about releasing 5-aminosalicylic acid from cellulose nanocrystals (CNCs) and CNC-chitosan hydrogels. The release profile of 5-aminosalicylic acid from CNC-chitosan hydrogel can be accurately represented by the Korsemeyar-Peppas equation.

Funding

This research was funded by Widya Mandala Surabaya Catholic University, grant number 260H/WM01.5/2023.

Acknowledgments

Strong support for using various research facilities in the Process Technology laboratory is appreciated.

Conflicts of Interest

The authors declare no conflict of interest.

References

1. Turanlı, Y.; Acartürk, F. Preparation and characterization of colon-targeted pH/Time-dependent nanoparticles using anionic and cationic polymethacrylate polymers. *Eur. J. Pharm. Sci.* **2022**, *171*, 106122, https://doi.org/10.1016/j.ejps.2022.106122.
2. Zhang, S.; Kang, L.; Hu, S.; Hu, J.; Fu, Y.; Hu, Y.; Yang, X. Carboxymethyl chitosan microspheres loaded hyaluronic acid/gelatin hydrogels for controlled drug delivery and the treatment of inflammatory bowel disease. *Int. J. Biol. Macromol.* **2021**, *167*, 1598-1612, https://doi.org/10.1016/j.ijbiomac.2020.11.117.
3. Zhang, S.; Kang, L.; Hu, S.; Hu, J.; Fu, Y.; Hu, Y.; Yang, X. Carboxymethyl chitosan microspheres loaded hyaluronic acid/gelatin hydrogels for controlled drug delivery and the treatment of inflammatory bowel disease. *Gels* **2022**, *8*, 155, https://doi.org/10.3390/gels8030155.
4. Shahdadi Sardo, H.; Saremnejad, F.; Bagheri, S.; Akhgari, A.; Afrasiabi Garekani, H.; Sadeghi, F. A review on 5-aminosalicylic acid colon-targeted oral drug delivery systems. *Int. J. Pharm.* **2019**, *558*, 367-379, https://doi.org/10.1016/j.ijpharm.2019.01.022.
5. Seyedian, S.S.; Nokhostin, F.; Malamir, M.D. A review of the diagnosis, prevention, and treatment methods of inflammatory bowel disease. *J. Med. Life* **2019**, *12*, 113-122, https://doi.org/10.25122/jml-2018-0075.
6. Ahmad, A.; Ansari, M.M.; Mishra, R.K.; Kumar, A.; Vyawahare, A.; Verma, R.K.; Raza, S.S.; Khan, R. Enteric-coated gelatin nanoparticles mediated oral delivery of 5-aminosalicylic acid alleviates severity of DSS-induced ulcerative colitis. *Mater. Sci. Eng. C* **2021**, *119*, 111582, https://doi.org/10.1016/j.msec.2020.111582.
7. Stavarache, C.E.; Ghebaur, A.; Dinescu, S.; Samoilă, I.; Vasile, E.; Vlasceanu, G.M.; Iovu, H.; Gârea, S.A. 5-Aminosalicylic Acid Loaded Chitosan-Carrageenan Hydrogel Beads with Potential Application for the Treatment of Inflammatory Bowel Disease. *Polymers* **2021**, *13*, 2463, https://doi.org/10.3390/polym13152463.
8. Song, J.; Li, X.; Niu, Y.; Chen, L.; Wei, Z.; Li, Y.; Wang, Y. pH-sensitive KHA/CMC-Fe^{3+}@CS hydrogel loading and the drug release properties of riboflavin. *Particuology* **2024**, *86*, 13-23, https://doi.org/10.1016/j.partic.2023.04.003.
9. Fereydouni, P.; Al Mohaddesin, A.; Khaleghi, S. Targeted biocompatible Zn-metal–organic framework nanocomposites for intelligent chemotherapy of breast cancer cells. *Sci. Rep.* **2024**, *14*, 18311, https://doi.org/10.1038/s41598-024-69457-6.
10. Xu, S.; Cai, J.; Cheng, H.; Wang, W. Sustained release of therapeutic gene by injectable hydrogel for hepatocellular carcinoma. *Int. J. Pharm.: X* **2023**, *6*, 100195, https://doi.org/10.1016/j.ijpx.2023.100195.
11. Taghizadeh, F.; Mehryab, F.; Mortazavi, S.A.; Rabbani, S.; Haeri, A. Thiolated chitosan hydrogel-embedded niosomes: A promising crocin delivery system toward the management of aphthous stomatitis. *Carbohydr. Polym.* **2023**, *318*, 121068, https://doi.org/10.1016/j.carbpol.2023.121068.
12. Lu, H.-T.; Lin, C.; Wang, Y.-J.; Hsu, F.-Y.; Hsu, J.-T.; Tsai, M.-L.; Mi, F.-L. Sequential deacetylation/self-gelling chitin hydrogels and scaffolds functionalized with fucoidan for enhanced BMP-2 loading and sustained release. *Carbohydr. Polym.* **2023**, *315*, 121002, https://doi.org/10.1016/j.carbpol.2023.121002.
13. Gao, R.; Xu, S.; Chen, C.; Liu, D.; He, Y.; Zang, Y.; Dong, X.; Ma, G.; Liu, H. Impact of 1,25-dihydroxyvitamin D_3 PLGA-nanoparticles/chitosan hydrogel on osteoimmunomodulation. *Int. J. Biol. Macromol.* **2023**, *247*, 125624, https://doi.org/10.1016/j.ijbiomac.2023.125624.
14. Shan, H.; Yin, W.; Wen, L.; Mao, A.; Lang, M. An injectable thermo-sensitive hydrogel of PNICL-PEG-PNICL block copolymer as a sustained release carrier of EGCG. *Eur. Polym. J.* **2023**, *195*, 112214, https://doi.org/10.1016/j.eurpolymj.2023.112214.
15. Gong, F.; Jiang, L.; Gao, Y.; Xu, J.; Wang, T. Delivery of soluble ethinylestradiol complex by pH-responsive core-shell composite hydrogel capsules. *J. Appl. Polym. Sci.* **2023**, *140*, e54225, https://doi.org/10.1002/app.54225.
16. Putro, J.N.; Edi Soetaredjo, F.; Irawaty, W.; Budi Hartono, S.; Santoso, S.P.; Lie, J.; Yuliana, M.; Widyarani; Shuwanto, H.; Wijaya, C.J.; Gunarto, C.; Puspitasari, N.; Ismadji, S. Cellulose Nanocrystals (CNCs) and Its Modified Form from Durian Rind as Dexamethasone Carrier. *Polym*ers **2022**, *14*, 5197, https://doi.org/10.3390/polym14235197.
17. Sampath, U.G.T.M.; Ching, Y.C.; Chuah, C.H.; Singh, R.; Lin, P.-C. Preparation and characterization of nanocellulose reinforced semi-interpenetrating polymer network of chitosan hydrogel. *Cellulose* **2017**, *24*, 2215-2228, https://doi.org/10.1007/s10570-017-1251-8.

18. Udeni Gunathilake, T.M. S.; Ching, Y.C.; Chuah, C.H. Enhancement of Curcumin Bioavailability Using Nanocellulose Reinforced Chitosan Hydrogel. *Polym*ers **2017**, *9*, 64, https://doi.org/10.3390/polym9020064.
19. Yang, T.; Li, X.; Xu, N.; Guo, Y.; Liu, G.; Zhao, J. Preparation of cellulose nanocrystals from commercial dissolving pulp using an engineered cellulase system. *Bioresour. Bioprocess.* **2023**, *10*, 42, https://doi.org/10.1186/s40643-023-00658-z.
20. Moradi, M.R.; Salahinejad, E.; Sharifi, E.; Tayebi, L. Controlled drug delivery from chitosan-coated heparin-loaded nanopores anodically grown on nitinol shape-memory alloy. *Carbohydr. Polym.* **2023**, *314*, 120961, https://doi.org/10.1016/j.carbpol.2023.120961.
21. Korake, S.; Bothiraja, C.; Pawar, A. Design, development, and in-vitro/in-vivo evaluation of docetaxel-loaded PEGylated solid lipid nanoparticles in prostate cancer therapy. *Eur. J. Pharm. Biopharm*. **2023**, *189*, 15-27, https://doi.org/10.1016/j.ejpb.2023.05.020.
22. Lin, Y.-S.; Lin, K.-S.; Mdlovu, N.V.; Kung, P.-Y.; Jeng, U.S. Thermal-/pH-triggered hollow mesoporous carbon nanocarrier for NIR-responsive drug release. *Biomater. Adv.* **2023**, *151*, 213477, https://doi.org/10.1016/j.bioadv.2023.213477.
23. Dave, P.N.; Macwan, P.M.; Kamaliya, B. Biodegradable Gg-*cl*-poly(NIPAm-*co*-AA)/-*o*-MWCNT based hydrogel for combined drug delivery system of metformin and sodium diclofenac: *in vitro* studies. *RSC Adv.* **2023**, *13*, 22875-22885, https://doi.org/10.1039/D3RA04728H.
24. Amrabadi, T.; Jalilnejad, E.; Ojagh, S.M.A.; Vahabzadeh, F. Application of TOPSIS algorithm in describing bacterial cellulose-based composite hydrogel performance in incorporating methylene blue as a model drug. *Sci. Rep.* **2013**, *13*, 2755, https://doi.org/10.1038/s41598-023-29865-6.
25. Shakoor, I.F.; Pamunuwa, G.K.; Karunaratne, D.N. efficacy of alginate and chickpea protein polymeric matrices in encapsulating curcumin for improved stability, sustained release and bioaccessibility. *Food Hydrocoll. Health* **2023**, *3*, 100119, https://doi.org/10.1016/j.fhfh.2023.100119.